Acta Cryst. (1998). B**54**, 399–416

Centrosymmetric or Noncentrosymmetric? Case Study, Generalization and Structural Redetermination of $Sr_5Nb_5O_{17}$

S. C. Abrahams,[a]*† H. W. Schmalle,[b] T. Williams,[c] A. Reller,[d] F. Lichtenberg,[e] D. Widmer,[f] J. G. Bednorz,[f] R. Spreiter,[g] Ch. Bosshard[g] and P. Günter[g]

[a]*Institut für Kristallographie der Universität Tübingen, Charlottenstrasse 33, D-72070 Tübingen, Germany, and Physics Department, Southern Oregon University, Ashland, OR 97520, USA,* [b]*Institute for Inorganic Chemistry, University of Zürich, Winterthurerstrasse 190, CH-8057 Zürich, Switzerland,* [c]*JASCO International Co. Ltd, 4-21 Sennin-cho 2-chome, Hachioji City, Tokyo 193, Japan,* [d]*Inorganic and Applied Chemistry, University of Hamburg, Martin-Luther-King-Platz 6, D-20146 Hamburg, Germany,* [e]*Institut für Physik, EKM, Universität Augsburg, D-86135 Augsburg, Germany,* [f]*IBM Research Division, Zürich Research Laboratory, CH-8803 Rüschlikon, Switzerland, and* [g]*Institut für Quantenelektronik, ETH Hönggerberg, CH-8093 Zürich, Switzerland. E-mail: sca@mind.net*

(*Received 14 May 1997; accepted 16 December 1997*)

Abstract

The possibility that the structure of the novel semiconducting perovskite-related material strontium niobium oxide, $Sr_5Nb_5O_{17}$, refined by Schmalle *et al.* [*Acta Cryst.* (1995), C**51**, 1243–1246] in space group *Pnn*2, might instead belong to space group *Pnnm* has been investigated following an analysis of the atomic coordinates that indicated the latter space group to be more likely. All I_{obs} were carefully remeasured, first those within a hemisphere containing c^*, then all that lay within the full sphere of reflection. Refinement was undertaken, with each of two different sets of weights, in each space group. Each data set was used under three limiting intensity conditions: $I_{obs} > 4\sigma(I_{obs})$, $I_{obs} > 2\sigma(I_{obs})$ and finally with *all* reflections, but setting magnitudes with $I_{obs} \leq 0$ equal to 0. Fourteen separate tests based only upon the X-ray diffraction data may be used to distinguish between *Pnn*2 and *Pnnm*. Nine tests favored the latter choice, four were indeterminate and one was not used. Seven further tests may be made on the basis of physical measurement; of these, three strongly indicated *Pnnm*, one was indeterminate and three could not be used. The evidence clearly suggests the space group is *Pnnm*. The use of all reflections, including those with negative magnitude set equal to zero, is essential to avoid ambiguity in the X-ray diffraction tests and achieve the highest reliability. Refinement with weights based on variances of Type *A* and Type *B* [Schwarzenbach *et al.* (1995). *Acta Cryst.* A**51**, 565–569] resulted in improved reliability compared with that obtained from a popular empirical weighting scheme. The revised structure differs in several respects from that published previously.

1. Introduction

The structure of the novel semiconducting perovskite-related material strontium niobium oxide, $Sr_5Nb_5O_{17}$, was reported in space group *Pnn*2 by Schmalle *et al.* (1995), hereafter SWRLWB. Refinement of 2118 independent reflections gave final values of $R = 0.0387$ and $wR = 0.0449$. Examination of the atomic coordinates, to determine if they met the criteria for ferroelectricity (see, for example, Abrahams, 1996*a*), showed that all atoms are 0.11 Å or less from the mirror planes in *Pnnm* located at $z = 0$ or $\frac{1}{2}$, whereas the r.m.s. (root mean square) thermal and/or static atomic displacements of all atoms in the structure have magnitudes between 0.06 and 0.13 Å, see also §6. Since it is unlikely that a noncentrosymmetric structure would remain stable so close to centrosymmetry, it was decided to remeasure the diffraction data and redetermine the structure as reported below. It may be noted that the two octants of reciprocal space measured by SWRLWB, with common zonal reflections and bounded by $\theta_{max} = 30°$, did not include the potentially polar reciprocal axis as a diameter in their quadrant, thereby eliminating the possibility of measuring either Friedel or Bijvoet pairs.

A recent topical review by Marsh (1995) considers many of the problems associated with attempts at deciding 'by diffraction methods alone, whether a particular structure is centrosymmetric or only approximately so'. Marsh concludes that 'if a centrosymmetric description...provides adequate agreement between observed and calculated intensities, there is no profit in searching further'. Ferroelectric crystals are likely to be among the most difficult cases of this kind, since all atoms in ferroelectric materials are located within ~1 Å of a centrosymmetric arrangement (*cf.* Abrahams, 1996*a*).

A major recommendation in a report by a subcommittee of the IUCr Commission on Crystallographic

† Present address: Southern Oregon University.

Nomenclature (Schwarzenbach *et al.*, 1989) emphasized the importance of weak reflections in making the correct choice between a centrosymmetric and a noncentrosymmetric model. Schomaker & Marsh (1979) and Marsh (1981) had previously stressed the importance of this class of reflection when confronted with such a choice, and Kassner *et al.* (1993) presented a further demonstration of their value in resolving such space-group ambiguities. The critical importance, in eliminating systematic bias, of including all reflections in this task is explored further in the present paper, as is the evaluation of variance in calculating the combined standard uncertainties of the reflections.

Changes in a centrosymmetric structure as atoms undergo displacement under the influence of cooling may result in the elimination of all inversion centers present. Centrosymmetric arrays correspond thermodynamically to single-well potentials and noncentrosymmetric arrays in polar crystals to double-well potentials (*cf.* Tolédano & Tolédano, 1987). The barrier between such wells in the lower-temperature phase decreases in height as the transition temperature is approached, while the atomic thermal energy continues to increase, the two wells merging at this critical temperature. The properties of such noncentrosymmetric arrays in polar crystals are closely comparable to those in ferroelectric crystals.

In considering diffraction tests designed to distinguish between centrosymmetric and noncentrosymmetric crystals, Schomaker (1996) noted that a demonstration of deviations between atomic positions in the former and those in the latter as being unmeasurably small is not equivalent to proof that they are zero; he emphasized that this result shows only that the hypothesis of centrosymmetry has not been disproven. Since atomic displacements from centrosymmetry are likely to be infinitesimal only for infinitesimally small thermal displacements by all atoms present, at least some atomic displacements in the putative polar phase may be expected to exceed their r.m.s. thermal displacements. All known ferroelectric structures exhibit the expected polar properties, hence definitive measurement of candidate crystal properties provides unambiguous identification of noncentrosymmetry. If all allowed polar coefficients are found to be undetectably small, then the confidence with which the hypothesis of noncentrosymmetry is rejected is greatly increased.

In the following a series of 14 different tests based only on the diffraction data are presented that may allow a distinction to be made between centrosymmetric *Pnnm* and its corresponding polar space group *Pnn*2. Following Schomaker (1996), the results of successful diffraction tests are taken as providing consistency with those of physical tests rather than as independent proof. Seven physical tests available for physical confirmation are discussed, results from which offer a high level of confidence in the final space-group determination.

2. Crystal data

The preparation of $Sr_5Nb_5O_{17}$ is given by SWRLWB, who also report the unit cell to have a = 32.456 (5), b = 5.674 (2) and c = 3.995 (2) Å, V = 735.7 (6) Å^3, space group *Pnn*2 or *Pnnm*, Z = 2, $F(000)$ = 1062, D_x = 5.302 Mg m^{-3} for M_r = 1174.62. Black plate-like (100) crystals, grown by floating-zone melting, readily form elongated prisms by imperfect cleavage along (010) and (001).

3. Diffraction measurements

The original 0.035 × 0.135 × 0.387 mm black crystal used in the structure determination by SWRLWB was also the study crystal used in the following two new sets of intensity measurement.

3.1. *Data set 1*†

A hemisphere of reciprocal space with $0 < h < 58$, $-10 < k < 10$, $-7 < l < 7$ and θ_{max} = 39.9° was measured at 295 K by means of $\omega/2\theta$ scans with an Enraf–Nonius CAD-4 diffractometer. The scan angle was 0.90 + 0.35° tan θ, using graphite-monochromated Mo $K\alpha$ radiation with λ = 0.71073 Å. Each reflection was measured for a maximum time of 120 s, including those systematically absent. In addition to the Lorentz–polarization correction, a numerical absorption correction with T_{min} = 0.0648, T_{max} = 0.4829, based on six indexed crystal faces and μ = 21.8 mm^{-1}, was applied by Gaussian grid integration (Fair, 1990). The maximum variation detected in serial intensity measurement was 0.1%, on the basis of 3 standard reflections remeasured at 3 h intervals; crystal-orientation constancy was similarly checked following the measurement of each group of 400 I_{obs}. Of 9385 I_{obs}, 201 were standards and 446 were systematically absent reflections for a total of 9184 I_{obs}, including systematic absences.

The strong likelihood (see §1) that the use of reflections measured as very weak or negative would be effective in eliminating unwanted bias in the determination of centrosymmetry for the present case, in which any departure from centrosymmetry is necessarily small, led to the adoption of three limiting intensity conditions. Two were selected that bracket the commonly used limit $I_{obs} > 3\sigma(I_{obs})$, where $\sigma(I_{obs})$ is the uncertainty due only

† Lists of atomic coordinates, anisotropic displacement parameters, structure factors, agreement indicators, additional magnitudes of z and Δz in *Pnn*2, R^{free} values, correlation matrix coefficients, bond distances and bond valences, additional Nb—O and Sr—O bond lengths and bond angles, and figures showing the $N(z)$ distribution for data set 1 and the $\Sigma F_{obs}/\Sigma F_{calc}$ distributions of §7.1 have been deposited with the IUCr (Reference: BR0066). CIF depositions present refinement results based on data set 1 with each set of weights and also results based on data set 2 with each set of weights. Copies may be obtained through The Managing Editor, International Union of Crystallography, 5 Abbey Square, Chester CH1 2HU, England.

Table 1. *Agreement indicators for the three $Sr_5Nb_5O_{17}$ models refined with two data sets in Pnn2 and Pnnm*

Refined with weights derived from Type *A* and Type *B* variances, see §5.1. Condition (i) with $I_{obs} > 4\sigma(I_{obs})$. Condition (ii) with $I_{obs} > 2\sigma(I_{obs})$. Condition (iii) with all data, $I_{obs} < 0$ set = 0.

	*Pnn*2 Model I			Model II			*Pnnm*		
I_{obs} condition	(i)	(ii)	(iii)	(i)	(ii)	(iii)	(i)	(ii)	(iii)
Data set 1									
No. used	2093	2350	4543	2093	2350	4543	1117	1205	2509
R	0.0232	0.0264	0.1138	0.0232	0.0264	0.1138	0.0210	0.0224	0.0985
$wR(F^2)$	0.0559	0.0583	0.0891	0.0559	0.0583	0.0891	0.0527	0.0534	0.0775
S	0.996	0.960	1.022	0.996	0.960	1.023	0.969	0.952	0.856
Flack *x* parameter	0.53 (3)	0.53 (3)	0.50 (4)	0.50 (3)	0.48 (3)	0.50 (4)	—	—	—
Data set 2									
No. used	2528	2678	4556	2528	2678	4556	1350	1497	2515
R	0.0218	0.0231	0.0680	0.0217	0.0229	0.0680	0.0208	0.0227	0.0612
$wR(F^2)$	0.0570	0.0585	0.0693	0.0566	0.0577	0.0693	0.0569	0.0577	0.0661
S	1.090	1.034	0.946	1.084	1.046	0.945	1.183	1.134	0.940
Flack *x* parameter	0.51 (2)	0.51 (2)	0.51 (2)	0.48 (2)	0.48 (2)	0.48 (2)	—	—	—

to counting statistics and the third condition included *all* reflections.

Condition (i) considered only reflections with $I_{obs} > 4\sigma(I_{obs})$. Applying this condition to the 4804 [3956] resulting reflections, a total of 2291 [2093] I_{obs} remained if the space group were assumed to be *Pnn*2, in which case $I(hkl)$ and $I(h\bar{k}l)$ are averaged, where the first total is obtained with the first set of weights (see §5.1), while that in square parentheses is obtained with the second set (see also §5.1), and 1346 [1117] I_{obs} remained if the space group were assumed to be *Pnnm,* in which case $I(hkl)$, $I(h\bar{k}\bar{l})$, $I(hk\bar{l})$ and $I(\overline{hk}l)$ are averaged, see also Table 1S.† It may be noted that 7087 [7017] reflections had $I_{obs} > 0$.

Condition (ii), which considered only data with $I_{obs} > 2\sigma(I_{obs})$, resulted in a total of 5482 [4446] reflections, of which 2680 [2350] I_{obs} remained after averaging on the assumption that the space group is *Pnn*2, and a total of 1606 [1205] I_{obs} remained after averaging in *Pnnm*.

Condition (iii), that all $I_{obs} \leq 0$ be set equal to zero, yielded 8738 [8738] $I_{obs} \geq 0$ with 2509 [2509] unique reflections on averaging in *Pnnm* and 4543 [4543] on averaging in *Pnn*2, see Table 1; $R_{int}(I_{obs})$ = 0.0688 [0.0717], $R\sigma(I_{obs})$ = 0.0450 [0.0641] in the former and $R_{int}(I_{obs})$ = 0.0604 [0.0551], $R\sigma(I_{obs})$ = 0.0632 [0.0641] in the latter space group, where $R\sigma(I_{obs})$ is defined as $\Sigma[\sigma(I_{obs})]/\Sigma(I_{obs})$.

3.2. *Data set 2*

These reflections, obtained by measurement of the full reciprocal sphere, had $-58 < h < 58$, $-10 < k < 10$, $-7 < l < 7$ and $\theta_{max} = 39.9°$. The maximum time spent per reflection in set 2 was decreased to 80 s, with zero time spent on the systematically absent reflections, *cf.* §3.1. Data set 2 was measured in response to a recommendation by Flack (1996) 'to have any chance of distinguishing between *Pnn*2 and *Pnnm*, Friedel opposites, $I(hkl)$ and $I(\overline{hkl})$, are needed. $I(hkl)$ and $I(hk\bar{l})$ will not do'. This advice assumes a smaller residual absorption error in Friedel reflection pairs than in Bijvoet pairs. Data averaging in *Pnn*2, however, necessarily results in approximately equal numbers of comparably corrected Friedel and Bijvoet pairs; both sets were hence used in the following analyses.

All other measurement variables for data set 2 were identical to those for data set 1, resulting in 17 732 reflections, of which 318 were standards, yielding a total of 17 414 [17 414] unmerged reflections with $I_{obs} \geq 0$. 11 067 [9530] of these reflections were consistent with condition (i) and 12 287 [10 095] with condition (ii); 2515 [2515] unique I_{obs} remained after averaging in *Pnnm* under condition (iii), 1933 [1497] under condition (ii) and 1703 [1350] under condition (i); in *Pnn*2, 4556 [4556] I_{obs} remained for condition (iii), 3315 [2678] for condition (ii) and 2893 [2528] for condition (i), see also Table 1S. R_{int} (I_{obs}) = 0.0672 [0.0649], $R\sigma(I_{obs})$ = 0.0275 [0.0409] on averaging in *Pnnm* and $R_{int}(I_{obs})$ = 0.0653 [0.0621], $R\sigma(I_{obs})$ = 0.0379 [0.0409] on averaging in *Pnn*2. The departure of $R\sigma(I_{obs})/R_{int}(I_{obs})$ from unity indicates underestimation of $\sigma(I_{obs})$. All 17 414 unique reflections were averaged under condition (iii) for refinement with the beta version of *SHELXL*96 (Sheldrick, 1996*a*). It is notable that data set 2 contains more significant reflections under criterion (i) and (ii) than data set 1.

4. Physical measurements

4.1. *Pyroelectric p_3 coefficient*

Single crystals of point group *mm*2 have a single pyroelectric p_3 coefficient. The largest crystal available was of the dimensions ~1.3 × 0.4 × 0.07 mm, with the *c* axis parallel to the longest dimension and the *a* axis normal to the plate; (100) was highly reflective. The

† Tables 1S, 2(*a*), 2(*b*) and 2(*c*)S, 3S, 4S, 5(*a*) and 5(*b*)S, 6(*a*) and 6(*b*)S, 7S, C1–C4, and Figs. 1(*a*), 1(*b*) and 1(*c*)S, 2(*a*), 2(*b*) and 2(*c*)S, 3(*a*), 3(*b*) and 3(*c*)S have been deposited; see deposition footnote on p. 400.

small crystal was secured with adhesive to a microscope slide. Crystal surfaces closest to (001) were electroded with flexible silver ink (Engelhard, 1995); conductive strips connected these surfaces to opposite edges of the slide and thence to Cu conductors leading to a Keithley Model 6517 electrometer (sensitivity, 10 fC). The charge, if any, produced on changing the temperature of the crystal ~20 K was determined as ≤ 5 pC, hence p_3 is $\leq 8\ \mu C\ m^{-2}\ K^{-1}$. A crystal with a cross section of $\sim 1\ mm^2$ normal to *c*, if available, would reduce this upper limit by a factor of ~1/35. Comparable measurement of p_3 in α-$LiIO_3$ under identical conditions gave excellent agreement ($10\ \mu C\ m^{-2}\ K^{-1}$) with that in the compilation of Bhalla & Liu (1984). The pyroelectric coefficient magnitudes for both ferroelectric and nonferroelectric inorganic pyroelectrics in that compilation range from 0.4 (for ZnS) to 6200 $\mu C\ m^{-2}\ K^{-1}$ (for $Ba_{0.35}Sr_{0.65}Nb_2O_6$). It may be noted that if the space group were *Pnn*2, then as-grown crystals of $Sr_5Nb_5O_{17}$ would likely contain ferroelectric domains, thereby resulting in reduced effective magnitudes for the p_i coefficients.

4.2. *Piezoelectric d_{31} coefficient*

The point group *Pnn*2 has five independent piezoelectric d_{ij} coefficients. The fragility of the crystal in §4.1 to the application of stress along **c** precludes measurement of d_{33}; stress applied normal to the plate, however, would produce a charge through the coefficient d_{31} in the noncentrosymmetric space group. Compressive stress of $\sim 10^4\ N\ mm^{-2}$ resulted in an undetectable charge with the upper limit ~10 pC, hence $d_{31} \leq 0.001\ pC\ N^{-1}$. Values reported for d_{31} in materials with point group *mm*2 range from $12\ pC\ N^{-1}$ for $AgNa(NO_2)_2$ to $0.4\ pC\ N^{-1}$ for $KB_5O_8.4H_2O$ (Cook, 1984).

4.3. *Second harmonic generation*

The generation and detection of second harmonics by a laser beam incident on a given material provides unambiguous proof that the material is without inversion centers, *i.e.* is noncentrosymmetric (*e.g.* see Abrahams, 1972). Measurements were made on a polycrystalline sample of ~90 mg $Sr_5Nb_5O_{17}$, using equipment comparable to that described by Kurtz & Perry (1968) and Dougherty & Kurtz (1976). Intense pulses of light (15 mJ, 11 ps) from a pulsed (10 Hz) Nd-YLF laser with $\lambda = 1047$ nm were passed through the sample. If $Sr_5Nb_5O_{17}$ were noncentrosymmetric, frequency doubling would generate green light with $\lambda = 523.5$ nm. Detection of frequency-doubled light generated by the sample, if any, was undertaken in reflection by the use of an interference filter and photomultiplier, with transmission set at the second harmonic frequency.

$Sr_5Nb_5O_{17}$ produced low intensity white light in the laser beam, the intensity of which was 11% of that from crystalline quartz in the green wavelength region. The intensity at $\lambda = 523.5$ nm was indistinguishable (*i.e.* without intensity enhancement) from that at unrelated but nearby frequencies within the broad spectral range produced, hence this intensity may be taken as the upper limit of possible but undetected second harmonics. Quartz is the usual reference material since it generates so weakly. Although negative, unlike positive, results are not unambiguous, this comparison shows that if $Sr_5Nb_5O_{17}$ generates second harmonics, it must have an optical second-order nonlinear dielectric susceptibility less than 11% of that of quartz, for which $d_{11} = 0.503 \times 10^{-12}\ V^{-1}$ m. By comparison, $d_{31} = -7.1 \times 10^{-12}\ V^{-1}$ m in α-$LiIO_3$ and $d_{31} = 134 \times 10^{-12}\ V^{-1}$ m in GaAs; the materials SiO_2, α-$LiIO_3$ and GaAs are standards used to convert relative to absolute second-order nonlinear dielectric susceptibilities (Jerphagnon *et al.*, 1984).

4.4. *Calorimetry*

A noncentrosymmetric crystal that is close to centrosymmetry at a given temperature may confidently be expected, on grounds of thermodynamic stability and energy minimization, to undergo a transition to the centrosymmetric phase at higher temperatures, provided it neither melts nor decomposes. Accordingly, a search for such a phase transition was undertaken using a Netzsch STA 409 combined thermobalance/differential scanning calorimeter coupled to a BALZERS QMS 421 mass spectrometer. This combination allows the simultaneous detection of all possible changes in the sample over the temperature range most likely to include phase transitions or redox processes. Measurements on a 28.89 mg sample were carried out in an atmosphere of N_2 from 303 to 773 K at a rate of $2\ K\ min^{-1}$ to avoid the possibility of reoxidizing $Sr_5Nb_5O_{17}$ to $Sr_5Nb_5O_{17.5}$, *i.e.* to fully oxidized $Sr_2Nb_2O_7$. As shown in Fig. 1, neither indication of phase transition nor oxidation was observed in this temperature range. Comparable measurement in air or O_2 confirms the process of oxidation to thermodynamically stable $Sr_2Nb_2O_7$. A slight drift in mass is

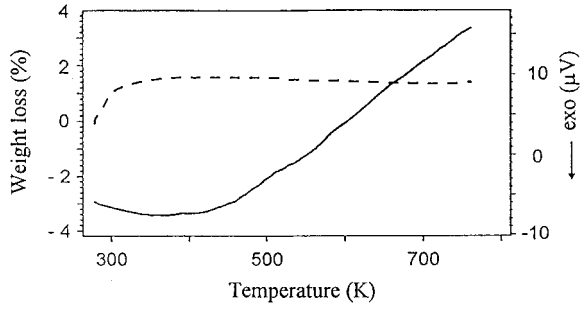

Fig. 1. Differential scanning calorimetric and thermogravimetric temperature dependence between 273 and 775 K. The solid line presents the former, the dashed line the latter, measurements.

Table 2. *Magnitudes of z and Δz (Å) from four separate refinements assuming space group Pnn2*

Refinements based on intensity condition (iii) with Type *A* and Type *B* variances. Since z(Model I) = 1 − z(Model II), the sign of each Δz in model II must be reversed for comparison with that in model I. Model II: $\Delta z = z - 0$ or $z - \frac{1}{2}$, depending on the plane closest to the given atom.

	Set 1, Model I		Set 1, Model II		Set 2, Model I		Set 2, Model II	
	z	Δz	z	Δz	z	Δz	z	Δz
Nb1	0.5000	0.000 (6)	0.4999	−0.001 (6)	0.5021	0.008 (3)	0.4981	−0.008 (3)
Nb2	0.5001	0.001 (5)	0.4999	−0.001 (5)	0.5003	0.002 (2)	0.4997	−0.001 (2)
Nb3	0.4997	−0.001 (5)	0.5003	0.001 (5)	0.5002	0.002 (2)	0.4994	−0.002 (2)
Sr1	0.4999	−0.001 (6)	0.5000	0.000 (6)	0.5014	0.006 (3)	0.4986	−0.006 (3)
Sr2	0.0006	−0.002 (8)	−0.0005	0.002 (8)	0.0040	0.016 (5)	−0.0039	−0.016 (5)
Sr3	−0.0001	−0.001 (5)	−0.0002	0.001 (5)	0.0028	0.011 (3)	−0.0028	−0.011 (3)
O1	0.5031	0.01 (3)	0.4957	−0.02 (4)	0.4853	−0.06 (2)	0.5148	0.06 (2)
O2	0.5105	0.04 (3)	0.4902	−0.04 (3)	0.5036	0.01 (1)	0.4963	−0.01 (1)
O3	−0.0044	−0.02 (6)	0.0050	0.02 (6)	−0.0002	−0.00 (3)	−0.0006	−0.00 (4)
O4	0.0111	0.04 (3)	−0.0106	0.04 (3)	−0.0066	−0.03 (2)	0.0058	−0.02 (2)
O5	0.0063	0.03 (2)	−0.0067	−0.03 (2)	0.0066	0.03 (2)	−0.0066	−0.03 (2)
O6	0.0218	0.09 (4)	−0.0248	−0.10 (4)	−0.0123	−0.05 (2)	0.0119	0.05 (2)
O7	0.5139	0.06 (3)	0.4863	−0.06 (3)	0.4906	−0.04 (2)	0.5093	0.04 (2)
O8	−0.0172	−0.07 (2)	0.0173	0.07 (2)	−0.0022	−0.01 (2)	0.0026	0.01 (2)
O9	−0.0188	−0.08 (2)	0.0182	0.07 (2)	0.0038	0.02 (2)	−0.0028	−0.01 (2)

normal with the thermobalance and the loss of ∼1.8% seen in Fig. 1, which is complete by ∼373 K, is attributable to the elimination of absorbed water vapor.

5. Refinement of the structure

5.1. *General*

Weights were assigned to each $(F_{obs})^2$ magnitude by two different methods. The first followed a commonly used procedure, based in the present case on the relationship in the beta-version of *SHELXL*96 (Sheldrick, 1996*a*): $w(F_{obs})^2 = q/[\sigma^2(F_{obs})^2 + (aP)^2 + bP + d + e\sin\theta]$, where $\sigma^2(F_{obs})^2$ is the variance in $(F_{obs})^2$ given by counting statistics; P = [f maximum of (0 or $(F_{obs})^2$) + $(1 - f)(F_{calc})^2$]/3; $q = 1$ when $c = 0$, or $\exp\{c[(\sin\theta)/\lambda]^2\}$ when c is positive, or $1 - \exp\{c[(\sin\theta)/\lambda]^2\}$ when c is negative; and the other constants are assigned values $a = 0.0268$, $b = 13.16$ for *Pnn*2 and 0.0210, 8.52 for *Pnnm* in data set 1, $a = 0.0284$, $b = 10.02$ for *Pnn*2 and 0.0180, 11.11 for *Pnnm* in data set 2 with $c = d = e = 0$ throughout.

The second set of weights was evaluated from estimates of the Type *A* and Type *B* variances, see Schwarzenbach *et al.* (1995). Statistically estimated Type *A* variances may be derived either from (*a*) the dispersion among equivalent reflections used in forming each averaged $(F_{obs})^2$ amplitude by means of Bessel's formula or (*b*) the averaged Poisson distribution of the individual amplitudes contributing to the average value of $(F_{obs})^2$, taking the symmetry equivalents appropriate for each choice of space group; the larger of (*a*) or (*b*) is then taken. Type *B* variances are based on nonstatistical information. The maximum uncertainty in the absorption correction was derived from the largest uncertainty in the linear dimensions of the crystal (see §3), estimated as 3%, leading to a variance of 9×10^{-4} $(F_{obs})^2$; evaluation of the remaining analogous uncertainties led to a final Type *B* variance of 30×10^{-4} $(F_{obs})^2$, *cf.* Abrahams (1969). The positive square root of the sum of the individual Type *A* and Type *B* variances yields the combined standard uncertainty (c.s.u.), *i.e.* $u_c(F_{obs})^2 = [\Sigma u^2(F_{obs})^2]^{1/2}$, where each $u(F_{obs})^2$ results from a Type *A* or Type *B* evaluation of standard uncertainty, with $w(F_{obs})^2 = 1/\Sigma u_c^2(F_{obs})^2$. In most cases the Type *A* variance is larger than Type *B*, the latter becoming negligible for large c.s.u. values; the Type *B* contribution becomes more important at small c.s.u. values. Refined parameter values based on the second set of weights are given below in square parentheses following those based upon the first set. Possible improvements in the routine evaluation of combined standard uncertainties are under investigation.

In view of the probability that the space group is centrosymmetric rather than noncentrosymmetric, the SWRLWB model was refined by the least-squares method on the basis of data set 1 and, separately, data set 2 first in space group *Pnn*2, then in *Pnnm*; all refinements with one set of weights were repeated using the second set. If the space group were *Pnn*2, then an as-grown crystal would most likely contain ferroelectric domains; there is an approximately equal chance for each domain that the orientation of its polar axis is either parallel or antiparallel to the polar **c** axis in any other domain. Such a domain structure would be equivalent to any atom with coordinates xyz in a given unit cell having an equal chance of its coordinates being $xy\bar{z}$ in any other unit cell.

Two variants based on the SWRLWB model were hence refined, using the $(F_{obs})^2$ magnitudes averaged in *Pnn*2. The beta-version of the *SHELXL*96 program (Sheldrick, 1996*a*) was used with each data set, under conditions (i), (ii) and (iii), see §3, with each set of weights applied. The variant in which the Flack (1983) x

Table 3. *Atomic coordinates and equivalent isotropic displacement parameters ($\times 10^{-4}$ Å^2) of $Sr_5Nb_5O_{17}$ at 295 K in Pnnm, refined under condition (iii) with data set 2 (coordinates and parameters based on the first set of weights are followed by values based on the second set in square parentheses, see §5.1*

	x	*y*	*z*	U_{eq}
Nb1	1/2 [1/2]	1/2 [1/2]	1/2 [1/2]	38 (1) [36 (1)]
Nb2	0.32264 (1) [0.32264 (1)]	0.53323 (8) [0.53339 (5)]	1/2 [1/2]	54 (1) [52 (1)]
Nb3	0.40931 (1) [0.40930 (1)]	0.00527 (7) [0.00517 (5)]	1/2 [1/2]	40 (1) [38 (1)]
Sr1	0.21466 (2) [0.21455 (2)]	0.5632 (1) [0.56289 (7)]	1/2 [1/2]	152 (1) [150 (1)]
Sr2	1/2 [1/2]	0 [0]	0 [0]	85 (1) [86 (1)]
Sr3	0.41129 (2) [0.41131 (1)]	0.4996 (1) [0.49960 (5)]	0 [0]	83 (1) [82 (1)]
O1	0.5374 (1) [0.53747 (10)]	0.2269 (7) [0.2262 (4)]	1/2 [1/2]	133 (7) [119 (5)]
O2	0.4522 (1) [0.45213 (9)]	0.2691 (6) [0.2687 (4)]	1/2 [1/2]	88 (6) [86 (5)]
O3	1/2 [1/2]	1/2 [1/2]	0 [0]	149 (11) [154 (9)]
O4	0.2091 (2) [0.20899 (10)]	0.2975 (7) [0.2971 (5)]	0 [0]	141 (8) [136 (6)]
O5	0.1208 (1) [0.12097 (9)]	0.2077 (7) [0.2075 (4)]	0 [0]	85 (6) [78 (5)]
O6	0.1328 (2) [0.13281 (10)]	0.7233 (8) [0.7228 (5)]	0 [0]	195 (10) [183 (7)]
O7	0.2799 (1) [0.27975 (10)]	0.3159 (7) [0.3168 (4)]	1/2 [1/2]	102 (6) [99 (5)]
O8	0.3308 (1) [0.33088 (10)]	0.5047 (11) [0.5046 (6)]	0 [0]	177 (9) [172 (6)]
O9	0.4165 (1) [0.41635 (10)]	−0.0104 (9) [−0.0091 (5)]	0 [0]	146 (8) [144 (6)]

parameter approached zero is referred to as model I, that with *x* approaching unity as model II. Although it is generally preferable to start refinements with $x = 0.5$, it is of significance to show that, even with starting parameter values far from 0.5 based on earlier use of data set 1, refinement proceeded readily to ∼0.5 for either model or data set under intensity conditions (i), (ii) and (iii). However, shift-limiting restraints (damping) were necessary for all intensity conditions with either model and either set of weights in *Pnn*2 to achieve stable refinement over many cycles as the *x* value slowly approached 0.5, see also §5.2 and §5.3. Excluding the damping condition did not change parameter values significantly on further refinement, but all *z* coordinate uncertainties increased by a factor of 2–4, *cf.* §7.10.

The observation of 12 reflections in data set 1 with $(F_{obs})^2$ consistently much smaller than $(F_{calc})^2$ led to the use of the *SHELXL*96 (Sheldrick, 1996*a*) empirical extinction correction in both data sets. The factor applied to $(F_{calc})^2$ was $k\{1 + [10^{-3}x(F_{calc})^2\lambda^3]/\sin 2\theta\}^{-1}$, where *k* is the overall scale factor and the final coefficient $x = 43\ (2)\ [42\ (2)] \times 10^{-4}$ for data set 1 and $47\ (2)\ [44\ (2)] \times 10^{-4}$ for data set 2, with both sets used under intensity condition (iii).

5.2. *Refinement with data set 1*

Refinement of both models in space group *Pnn*2 with *SHELXL*96 (Sheldrick, 1996*a*) weights, under all three intensity conditions of §3.1, led to the indicators in Table 1S; indicators obtained with Type *A* and Type *B* variances as reciprocal weights are given in Table 1, with corresponding Flack (1983) *x* parameters listed in both tables. The maximum parameter shifts in the final refinement cycles with 126 variables, for each of the intensity conditions, ranged from 0.000 [0.000] to 0.001 [0.004] standard uncertainties, with $\Delta\rho_{max} = 5.1$ [4.6], $\Delta\rho_{min} = -3.7$ [−3.9] e Å^{-3}. The anisotropic atomic displacement parameters (ADP's) of several atoms were nonpositive definite in the final refinement cycles based upon each intensity condition, see also §5.4. Refined *z* coordinates for both models and each set of weights are given in Tables 2 and 2S.

Comparable refinement in space group *Pnnm*, see §3, led to the indicators in Tables 1 and 1S. Final maximum parameter shifts were less than 0.001σ, with $\Delta\rho_{max} = 5.4$ [4.3], $\Delta\rho_{min} = -4.0$ [−3.6] e Å^{-3}. The ADP's for all atoms in the centrosymmetric space-group refinement were positive definite, see §5.4. The high ratio of principal mean-square displacements for O6, with $U^3/U^1 = 14.46$ for the first set of weights and 14.28 for the second set, each obtained under condition (iii), may result from the remaining uncompensated intensity measurement error, see CIF deposition.† Full convergence was reached in the course of 16 least-squares cycles, with no need for damping factors.

5.3. *Refinement with data set 2*

The course of refinement with the full-sphere set of data followed that given in §5.2. Increasing the damping factor in space group *Pnn*2 increased the parameter *x* in model I, but was without significant change in *wR*2; final values of *x* for both models and weights together with resulting refinement indicators are given in Tables 1 and 1S. The maximum parameter shift in the final refinement cycle for *Pnn*2 with either model or intensity criterion was $0.007\ [0.003]\sigma$, with $\Delta\rho_{max} = 7.1$ [5.4], $\Delta\rho_{min} = -7.2$ [−4.9] e Å^{-3}, see also §8.

Refinement in *Pnnm* led to indicators as given in Tables 1 and 1S. The maximum parameter shift in the final refinement cycles for *Pnnm* was $0.000\ [0.000]\sigma$, with $\Delta\rho_{max} = 6.9$ [5.0], $\Delta\rho_{min} = -7.2$ [−4.5] e Å^{-3}. The ADP's for all atoms refined in *Pnnm* were positive definite, see §5.4.

† See deposition footnote on p. 400.

A total of 86 parameters were refined in space group *Pnnm* with data sets 1 and 2; similarly, 126 parameters were refined in space group *Pnn*2 with each data set. The final atomic coordinates and U_{eq} values in space group *Pnnm* are presented in Table 3.

5.4. *Atomic displacement parameters*

Refinement with data set 1 and *SHELXL*96 (Sheldrick, 1996*a*) weights in space group *Pnn*2, for either model, led to nonpositive definite (n.p.d.) ADP's in atoms O1, O2, O5 and O9 under condition (i), and O2, O5, O7, O8 and O9 under condition (ii); under condition (iii), atoms O2, O5, O8 and O9 have n.p.d. ADP's for model I, but only O5, O8 and O9 have n.p.d. ADP's for model II.† Fewer n.p.d. ADP's are observed with data set 2; under condition (i), atoms O2, O5, O8 and O9 in model I and only O5 and O9 in model II, with very small n.p.d. values for O8. For condition (ii), model I, atoms O2, O5, O7 and O8; in model II, O2 O7, O8 and O9; under condition (iii) with models I and II, only O8 and O9 have n.p.d. ADP's, while that of O7 is zero in both models.

The application of Type *A* and Type *B* weights to data set 1 results, under condition (i), in n.p.d. ADP's for atoms O2, O5 and O9; under condition (ii), in n.p.d. ADP's for O2, O4, O5, O8 and O9 for model I and for O2, O5 and O9 in model II; under condition (iii), in n.p.d. ADP's for O5, O8 and O9. Application to data set 2 results in O2 and O9 becoming n.p.d. in model I and O2, O7, O8 and O9 in model II under condition (i), whereas the ADP's of O5 in model I and O3 in model II are very small. Under condition (ii), the ADP's of O2, O5 and O9 in model I and O2, O7, O8 and O9 in model II are n.p.d., whereas under condition (iii) the ADP's of atoms O2 and O8 are n.p.d. in both models, while those of O5 in model I and O7 in model II are very small but positive.

All ADP's refined in space group *Pnnm* are positive definite with either data set or weights.

6. Atomic displacements from centrosymmetry in space group *Pnn*2

The final z coordinate values determined with either data set under condition (iii) for either model in space group *Pnn*2,† see also §5, are close to either 0 or $\frac{1}{2}$. All atoms in space group *Pnnm* lie on mirror planes with $z = 0$ or $\frac{1}{2}$. The magnitude of each z coordinate determined in *Pnn*2 and its distance from the nearest mirror plane is given in Table 2 for models I and II refined with Type *A* and Type *B* variances. For data set 1, O6 has the largest such difference at 0.10 (4) Å and for data set 2 it is 0.06 (2) Å for O1, without the use of damping in either case. The r.m.s. amplitude of thermal or static atomic displacement for O6 is 0.133 (11) Å and for O1 it is 0.103 (5) Å. Results based on refinement under the same conditions, but with Marquardt damping, are given in Table 2(*a*)S. The corresponding z coordinates and Δz magnitudes from refinement with the *SHELXL*96 (Sheldrick, 1996*a*) weights, both with and without damping, are presented in Tables 2(*b*)S and 2(*c*)S. It may be seen from Table 2(*b*)S that, with data set 1, the largest displacement is 0.051 (2) Å by O8, whereas with data set 2 it is 0.09 (3) Å by O6. The corresponding r.m.s. amplitude for O8 is 0.137 (5) Å, whilst that for O6 is 0.133 (5) Å. No parameter changed value significantly on lifting the restraints, but the uncertainty in all z coordinates increased by a factor of 2–4, as noted in §5.1. These results confirm the earlier conclusion drawn from the atomic coordinates refined by SWRLWB in space group *Pnn*2 that the atomic displacements from centrosymmetry by assuming this space group are either without significance or else are so much smaller than their r.m.s. amplitudes that the resulting structure would be thermodynamically unstable by comparison with the centrosymmetric structure. The original assumption that the space group of $Sr_5Nb_5O_{17}$ is noncentrosymmetric hence remained open to question prior to the choice made in §7.22.

† See deposition footnote on p. 400.

7. *Pnnm versus Pnn*2

Determination of the $Sr_5Nb_5O_{17}$ crystal structure illustrates many aspects common to studies in which difficulties are experienced in the course of making a choice between possible centrosymmetric or noncentrosymmetric space groups; it thereby provides a classical case study. Tests based only on diffraction results may often be ambiguous or misleading, as emphasized by Marsh (1995, 1996), but their easy accessibility has tended to continue their use. Many traditional tests based on diffraction data alone have been well summarized by Baur & Tillmanns (1986). The reliability of results obtained with 14 such tests on $Sr_5Nb_5O_{17}$, and a further seven tests based on physical measurement, are considered in §7.1–§7.22.

7.1. *Intensity distribution*

The use of statistical tests based on the probability distribution of the measured intensities has recently been discussed by Marsh (1995), who notes many instances in which they have misled authors. He concludes that diffraction methods alone cannot determine whether a particular structure is centrosymmetric or is only approximately so. The combination of condition (iii) and the small size of the crystal used in the present study results in many I_{obs} with magnitude less than $2\sigma(I_{obs})$ or $2u_c(I_{obs})$. The number of such I_{obs} is data-set-, weighting- and space-group-dependent after averaging; with data set 1 it ranges from 36 to 41% of the

total number of reflections for the first set of weights and from 48 to 53% for the second set. With data set 2, it ranges from 23 to 27% for the first set and is ~41% for the second set of weights. Although a smaller value of θ_{max} than the 40° used would have reduced the percentage of weak reflections, these data contain information of critical importance in space-group determination, as demonstrated hereafter.

Examination of the $N(z)$ cumulative probability distribution (Howells *et al.*, 1950) for $Sr_5Nb_5O_{17}$ in both data sets based on each of the three intensity conditions (see §3.1 and §3.2) shows that the totality of *all* data in either set [*i.e.* corresponding to condition (iii)] clearly follows that expected for a centric distribution. Fig. 2 shows the results for data set 2, those for data set 1 having been deposited.† In sharp contrast, the cumulative probability distribution of intensities remaining in data set 2 under condition (ii) is much closer to the acentric distribution in the sensitive low z value range; similarly, the intensities remaining under condition (i) coincide with the acentric distribution for $z \leq 1.3$. The importance of measuring and retaining the complete set of reflection intensities is hence demonstrable, leading to an $N(z)$ test that strongly favors the choice of *Pnnm*, whereas rejection of the weak or very weak intensities would lead to the false indication that the space group is noncentrosymmetric *Pnn*2.

7.2. *Hamilton R ratio*

Routine use of the Hamilton (1965) R-ratio test, not uncommon in earlier studies, has been deprecated by Marsh (1995) with good reason. Application of the method is examined here. An option in *SHELXL*96 (Sheldrick, 1996*a*) allows refinement of identical unmerged-reflection sets; the resulting R_{exp} = [$wR(F)$ for *Pnn*2]/[$wR(F)$ for *Pnnm*] for data sets 1 and 2, using each intensity condition of §3.1 and §3.2 with each of the possible space groups and the *SHELXL*96 (Sheldrick, 1996*a*) weights of §5.1, are given in Table 4. Corresponding R_{exp} values from refinement with merged reflections using weights derived from Type *A* and Type *B* variances are also given in Table 4. Refinement with *SHELXL*96 (Sheldrick, 1996*a*) is necessarily based on structure amplitudes; the $w(F_{obs} - F_{calc})$ magnitudes for the R-ratio test were hence obtained in part from the final refined parameters. The 126 parameters refined without restraint in *Pnn*2 and the 86 parameters similarly refined in *Pnnm* lead to the values $R_{b,n-m,\alpha}$ given in Table 4 at the 99.5% significance level under the hypothesis that the diffraction data is fitted better in space group *Pnn*2 than in *Pnnm*. One refinement series only, based on condition (iii) in data set 2 with *SHELXL*96 (Sheldrick, 1996*a*) weights, resulted in an experimental ratio R_{exp} that was significantly larger than $R_{b,n-m,\alpha}$ at this level, thereby supporting the hypothesis; since R_{exp} is less than $R_{b,n-m,\alpha}$ for all other entries in Table 4, however, these values reject the hypothesis. The Hamilton R-ratio test is hence indeterminate in the present case.

Baur & Tillmanns (1986) have noted that the number of observations n less the number of refined parameters m in modern single-crystal structure refinement, *i.e.* $n - m = b$, the number of degrees of freedom, often exceeds 1000, as in Table 4. As b increases further, they point out that the limit for improvement in R_{exp} becomes increasingly small. Higher experimental accuracy for larger values of b hence becomes necessary to avoid misleading indications by the R-ratio test.

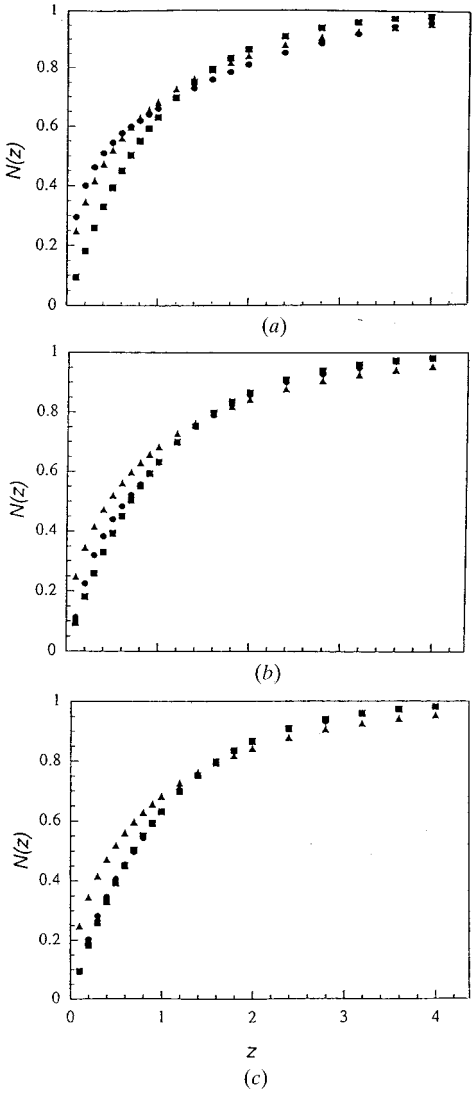

Fig. 2. The $N(z)$ cumulative probability distribution based on data set 2, (*a*) for intensity condition (iii), (*b*) for condition (ii) and (*c*) for condition (i), see §7.1. The symbol ● denotes the experimental, ■ the noncentrosymmetric and ▲ the centrosymmetric distributions.

† See deposition footnote on p. 400.

Table 4. *Hamilton R ratios, with α = 0.005, in space-group choice for $Sr_5Nb_5O_{17}$*

See §7.2 for discussion.

		Data set 1			Data set 2		
Intensity condition	b	$n-m$	$R_{b,n-m,\alpha}$	$R_{\rm exp}$	$n-m$	$R_{b,n-m,\alpha}$	$R_{\rm exp}$
*SHELXL*96 (Sheldrick, 1996*a*) weights							
(i)	40	4498	1.0074	0.9753	10 941	1.0030	0.9818
(ii)	40	5137	1.0065	0.9664	12 161	1.0027	0.9790
(iii)	40	8612	1.0039	1.0022	17 288	1.0019	1.0073
Type *A* and Type *B* weights							
(i)	40	1967	1.0170	0.9849	2402	1.0139	0.9876
(ii)	40	2224	1.0150	0.9743	2552	1.0131	0.9937
(iii)	40	4417	1.0075	1.0011	4430	1.0075	1.005

7.3. *Free R statistic*

The statistical quantity $R_{\rm test}^{\rm free}$, used to measure agreement between observed and calculated amplitudes for a test set of reflections that have been deliberately omitted from the refinement process (Brünger, 1992, 1993), was introduced primarily for distinguishing correct from incorrect configurations within macromolecules. Sheldrick (1996*b*) suggested it might also be used as a selection criterion for inversion centers. The results given in Table 3S show that $R_{\rm test}^{\rm free}$ for either data set, taking 10% of the total number of reflections as test reflections, is lower in *Pnnm* than in *Pnn*2 for all intensity conditions. This statistic, if the resulting difference of 0.9% in data set 1 and 2.2% in data set 2 under intensity condition (iii) is significant, hence favors the centrosymmetric space group. Sheldrick (1996*b*) assumes differences less than 0.5% to be without significance.

7.4. *Refinement efficiency*

A common test compares the efficiency with which the refinement of a given starting structure converges, using the least-squares method, in each candidate space group that differs only in the presence or otherwise of inversion centers. Convergence is expected to be more rapid in a correctly chosen space group than in an incorrect choice, since ill-conditioned normal equations lead readily to false minima. The number of refinement cycles needed to achieve convergence in *Pnn*2 was ∼90 for either data set, even with the help of large damping factors. By contrast, convergence was reached in *Pnnm* within 16 refinement cycles without the need for damping factors. Refinement in *Pnnm* is clearly more efficient and is hence suggestive of consistency with the correct space-group choice.

7.5. *Distribution of $\Sigma F_{obs}/\Sigma F_{calc}$ versus $\langle F\rangle$*

Kassner *et al.* (1993) introduced a new test for the detection or otherwise of inversion centers, based upon an expected larger number of departures of $\Sigma F_{\rm obs}/\Sigma F_{\rm calc}$ from unity and an increase in $\Sigma F_{\rm obs} - \Sigma F_{\rm calc}$ for the incorrect choice of space group. Upper Fig. 2(*a*)S shows the distribution for 27 [27] equally populated intervals of $\langle F\rangle$ from data set 1 based upon refinement in space group *Pnn*2, model I (values in parentheses refer to Type *A* and Type *B* variances); upper Fig. 2(*b*)S shows the distribution for space group *Pnn*2, model II; upper Fig. 2(*c*)S shows that for 25 [26] such intervals in space group *Pnnm*. The three lower Figs. 2(*a*)S, 2(*b*)S and 2(*c*)S present the corresponding distributions for 30 [30] equally populated intervals of $\langle F\rangle$ from data set 2 on refinement in *Pnn*2 and for 28 [28] such intervals in *Pnnm*. Figs. 3(*a*)S, 3(*b*)S and 3(*c*)S show the comparable distributions on refinement with weights based on Type *A* and Type *B* variances, see §5.1. Examination of the magnitudes in the upper Figs. 2(*a*)S, 2(*b*)S and 2(*c*)S shows that both $\Sigma F_{\rm obs}/\Sigma F_{\rm calc}$ and $\Sigma F_{\rm obs} - \Sigma F_{\rm calc}$ slightly favor *Pnnm*. In the lower Figs. 2(*a*)S, 2(*b*)S and 2(*c*)S $\Sigma F_{\rm obs}/\Sigma F_{\rm calc}$ slightly favors *Pnn*2, whereas $\Sigma F_{\rm obs} - \Sigma F_{\rm calc}$ slightly favors *Pnnm*. The distribution in Figs. 3(*a*)S, 3(*b*)S and 3(*c*)S shows that $\Sigma F_{\rm obs} - \Sigma F_{\rm calc}$ slightly favors *Pnn*2 with either data set, but that, to the contrary, $\Sigma F_{\rm obs}/\Sigma F_{\rm calc}$ slightly favors *Pnnm* with data set 2. The test is hence indeterminate in the present case.

7.6. *Anomalous scattering distribution*

Anomalous dispersion in noncentrosymmetric crystals results in $I(hkl) \neq I(\overline{hkl})$, whereas all symmetry-equivalent reflections remain equal in centrosymmetric crystals. The relative contribution of f' to $I(hkl)$ is larger in weaker than in stronger reflections in either case, since it is independent of scattering angle; a comparable contribution by f'' occurs only in noncentrosymmetric crystals. As the intensity of a reflection approaches zero, the chance of it being measured as negative increases. In the present study $f'(\mathrm{Sr}) = -1.53$, $f''(\mathrm{Sr}) = 3.25$, $f'(\mathrm{Nb}) = -2.07$, $f''(\mathrm{Nb}) = 0.62$, with both $f'(\mathrm{O})$ and $f'(\mathrm{O}) \simeq 0.1$. Averaging equivalent reflections by taking $\langle I\rangle = (1/n)\Sigma I_{\rm obs}$, including individual $I_{\rm obs} < 0$ at their full negative value with resulting $\langle I\rangle$ set to zero magnitude if it thereby becomes negative, results in an appreciable number of averaged reflections with reduced magnitude in either space group owing to the contribution of f'. In the case of noncentrosymmetric crystals the additional f'' contribution is expected to result in a further increase

Table 5. *Anomalous scattering effect on intensity ratios after averaging*

Ratio of number of averaged $I(hkl)_{obs}$ with $l \neq 0$ to number including $l = 0$.

	Intensity condition	Ratio in *Pnn*2	Ratio in *Pnnm*
Data set 1	(iii)†	0.896 [0.896]‡	0.896 [0.896]
	$I_{obs} > 1\sigma(I_{obs})$	0.889 [0.887]	0.898 [0.882]
	(ii)	0.886 [0.882]	0.894 [0.851]
	(i)	0.881 [0.880]	0.881 [0.855]
Data set 2	(iii)	0.896 [0.896]§	0.896 [0.896]
	$I_{obs} > 1\sigma(I_{obs})$	0.890 [0.889]	0.893 [0.882]
	(ii)	0.888 [0.885]	0.893 [0.876]
	(i)	0.885 [0.884]	0.887 [0.864]

† See §3.1 and §3.2 for intensity conditions (i), (ii) and (iii). ‡ Number of averaged reflections with $l \neq 0$ for data set 1 in *Pnn*2 under conditions (i), (ii) and (iii) is 2018 [1841], 2374 [2073] and 4070 [4070], in *Pnnm* it is 1073 [865], 1300 [928] and 2036 [2036], respectively; for $I_{obs} > 1\sigma(I_{obs})$, it is 2697 [2307] in *Pnn*2 and 1466 [1167] in *Pnnm*. Values based on the second set of weights are given in square parentheses. § Corresponding numbers for data set 2 in *Pnn*2 under conditions (i), (ii) and (iii) are 2559 [2235], 2945 [2369] and 4082 [4082]; in *Pnnm* they are 1370 [1057], 1564 [1188] and 2041 [2041], respectively; for $I_{obs} > 1\sigma(I_{obs})$, they are 3251 [2793] in *Pnn*2 and 1698 [1387] in *Pnnm*. All ratios for reflections averaged in *Pnnm* have been normalized to that in *Pnn*2 for condition (iii) by the factor 1.105 [1.103] for easier comparison.

in the number of weaker averaged reflections among members of Friedel and Bijvoet pairs, leading to a larger number of $\langle I \rangle$ with very weak or zero magnitude than in centrosymmetric crystals, see also §7.1.

A distinction between centrosymmetric and noncentrosymmetric crystals, based on the above effects, may hence be made by comparing the ratio of the total number of independent $F(hkl)$ reflections to the number with $l \neq 0$, after averaging both under the assumptions of centrosymmetry and noncentrosymmetry for each of the three intensity conditions used in §3.1 and §3.2. Reflections with $l = 0$ are insensitive to the possible presence of inversion centers. An additional intensity condition, in which only data with $I_{obs} > 1\sigma(I_{obs})$ are considered, was also used in this test for greater sensitivity. The experimental normalized ratios, see Table 5, decrease as expected from condition (iii) to (i). Examination reveals maximum differences of 2.9% for data set 1 and 2.4% for data set 2, between such ratios. However, corresponding differences between *Pnn*2 and *Pnnm* for the two conditions with the largest percentage of weak reflections vary between +1.0 and −0.8%. The possible contribution by f'' is hence small and no larger than that due to changing weights. The results in Table 5 are thus consistent with the centrosymmetric space group. Alternative formalisms for increasing the sensitivity of this test are under investigation.

7.7. *Measurement of individual Bijvoet or Friedel pairs*

Careful examination of individual reflection pairs that, in the case of noncentrosymmetric crystals with a polar c axis, would possess a Bijvoet [*e.g.* $I(hkl)$ and $I(hk\bar{l})$] or Friedel [*e.g.* $I(hkl)$ and $I(\overline{hkl})$] pair relationship provides a related but more direct means of determination, particularly if measured on an extended faceted single crystal (*cf.* Abrahams, 1975). Eight Bijvoet and eight Friedel pairs of reflections only in data set 2 have experimental intensity ratios that differ from unity by more than $3\sigma(I_{obs})$, assuming the symmetry to be *Pnn*2, although many others differ by more than $2\sigma(I_{obs})$. These 16 pairs were remeasured on the diffractometer, following careful reorientation of the study crystal, at 1/20 the speed previously used, thereby reducing the counting statistical contribution to $u_c(I_{obs})$ by a factor of ∼1/7–1/8. In data set 2, Friedel pairs $I(611)$ and $I(\overline{611})$ appeared to differ by 11.9%, whereas individual uncertainties based only on counting statistics were ∼2.2%. Careful remeasurement reduced this apparent difference to an insignificant 0.2%, see Table 6. Initial inspection of this table may suggest differences between Bijvoet pairs greater than those between Friedel pairs; closer examination, however, reveals comparable differences with equivalent non-Bijvoet or non-Friedel reflections. The differences are hence without significance at the present accuracy level and the test should be regarded as indeterminate. Realistic standard uncertainties are clearly larger than those given in Table 6.

7.8. *Synchrotron radiation*

Selection of synchrotron X-rays with a wavelength close to the Nb or Sr K or L absorption edges would enhance differences in intensity between Bijvoet or Friedel pairs of reflections in noncentrosymmetric crystals by increasing the value of f'' relative to f and f'. The intensity ratio of selected pairs as the wavelength is systematically varied through the edge is constant in centrosymmetric crystals, but is expected to vary significantly in noncentrosymmetric crystals, unless twinning produces pseudoinversions. Neither this test nor the selected short wavelength synchrotron radiation test utilized by Kassner *et al.* (1993), in choosing between space groups *Cc* and *C*2/*c* to minimize absorption effects, were used in the present study.

Table 6. *Comparison of Bijvoet and Friedel reflection-pair corrected intensities in $Sr_5Nb_5O_{17}$ assuming space group Pnn2*

hkl	I_{obs}	$\sigma(I_{obs})$	*hkl*	I_{obs}	$\sigma(I_{obs})$
$\overline{6}11$	247.8	0.7	$12,2\bar{2}$	231.8	0.2
$\overline{6}1\bar{1}$	248.2	0.7	$\overline{12},22$	239.2	0.3
$61\bar{1}$	259.2	0.7	$12,22$	229.2	0.3
$\overline{6}11$	260.2	0.7	$\overline{12},\overline{22}$	228.7	0.3
$10,22$	199.7	0.2	$18,15$	60.0	0.3
$\overline{10},\overline{22}$	197.5	0.2	$\overline{18},\overline{15}$	52.4	0.3
$10,2\bar{2}$	203.8	0.2	$18,1\bar{5}$	53.5	0.3
$\overline{10},\bar{2}2$	201.9	0.2	$\overline{18},\bar{1}5$	54.2	0.3
$17,1\bar{2}$	67.8	0.2	$22,4\bar{2}$	113.8	0.2
$\overline{17},\bar{1}2$	69.3	0.2	$\overline{22},\bar{4}2$	118.5	0.3
$17,12$	70.2	0.2	$22,42$	117.1	0.3
$\overline{17},\overline{12}$	69.8	0.2	$\overline{22},\overline{42}$	118.3	0.3
$16,53$	83.8	0.2	$34,22$	116.5	0.3
$\overline{16},\overline{53}$	81.7	0.2	$\overline{34},\overline{22}$	114.0	0.3
$16,5\bar{3}$	80.4	0.2	$34,2\bar{2}$	113.5	0.3
$\overline{16},\bar{5}3$	82.2	0.2	$\overline{34},\bar{2}2$	117.2	0.3

The s.u. contains only the counting statistics contribution.

7.9. *Correlation matrix coefficients*

Major differences between the magnitudes of the correlation matrix coefficients resulting from refinement in candidate space groups are sometimes used as a determinant of space-group choice. Refinement of a structural parameter that in fact should not be varied is expected to result in an increased correlation coefficient, usually by interaction with an ADP for the same atom. Correlation matrix coefficients greater than 0.5 resulting from refinement with each data set under each intensity condition, using each set of weights and in each space group, for a total of 12 separate refinement conditions, are given in Table 4S; coefficients in this table for refinement in space group *Pnn*2 are those obtained both with and without the application of restraints.

It is notable that the largest coefficients in space group *Pnnm* are less than 0.7 for any refinement condition and always relate the extinction parameter to the overall scale factor. All other coefficients in *Pnnm* are less than 0.5. By contrast, the largest coefficients in space group *Pnn*2 exceed 0.9 under all refinement conditions in the absence of applied restraints; if restraints are applied, these coefficients are thereupon reduced to values less than 0.55. The comparison is only valid as a test, however, in the absence of restraints. All very large coefficients in space group *Pnn*2 are of the form $U^{33}(On)/z(On)$, where n = 1 or 3–9, or the form $U^{ij}(On)/U^{jk}(On)$, where *ij,jk* is typically 13,33 or 12,13 or 22,23 for many of the same atoms.

The choice of space group is unlikely to influence either extinction parameter or overall scale factor strongly, hence a large mutual correlation is probably not a reliable indicator of unusual interaction. However, the increased correlation coefficient magnitudes of the form $U^{33}(O)/z(O)$ or $U^{ij}(O)/U^{jk}(O)$ for many O atoms in *Pnn*2, in comparison with their much smaller values in *Pnnm*, are strongly suggestive of the centrosymmetric space group as the more likely choice.

7.10. *Standard uncertainties*

Standard uncertainties larger than expected in whole classes of parameters may also be indicators of incorrectly assigned symmetry elements (Baur & Tillmanns, 1986). Such behavior is often related to unusually large correlation coefficients. R.m.s. uncertainties over all atomic positions are 0.0060 [0.0047] and 0.0051 [0.0034] Å, respectively, for data sets 1 and 2 with *SHELXL*96 (Sheldrick, 1996*a*) weights in *Pnnm*, excluding those that are necessarily zero by symmetry, and are 0.0297 [0.0261] and 0.0231 [0.0162] Å, respectively, in *Pnn*2. The uncertainties increase by a factor of *ca.* five in either data set on refinement in the polar space group under condition (iii). It may be noted that the s.u. of 0.024 Å for the sensitive Nb1—O3 bond length in space group *Pnn*2 becomes reduced to an s.u. of 0.001 Å for the same atom in space group *Pnnm* under the same refinement conditions. The standard uncertainties in equivalent isotropic ADP's lie within the range 0.0001–0.0010 $Å^2$ for either data set in space group *Pnnm*, with almost the same range for comparable conditions in space group *Pnn*2. The s.u.'s of all z(O) coordinates refined in space group *Pnn*2 are larger than those of the equivalent x(O), y(O) coordinates by a factor of 2.4–8.9 [2.8–9.9] for data set 1 and 3.7–8.6 [5.2–8.8] for data set 2. The observed differences in the ADP s.u.'s are not determinate; however, differences in atomic coordinate s.u.'s, particularly for the sensitive z(O), strongly favor the centrosymmetric space-group choice.

7.11. *Largest final parameter-shift to standard uncertainty ratio*

The ratio of the largest final parameter-shift to its standard uncertainty (l.f.p.s.t.s.u.), obtained on completing refinement in a given space group compared with that obtained for another space group, may also be used as a determinant between the two. The l.f.p.s.t.s.u. ratio for each intensity condition in *Pnnm* ranges from −0.001 to 0.001 for either data set, whereas each magnitude increases by two to three orders on refinement in *Pnn*2 with *SHELXL*96 (Sheldrick, 1996*a*) weights under all intensity conditions in either data set; the corresponding increase in l.f.p.s.t.s.u. ratio on refinement using Type *A* and Type *B* variances is an order of magnitude less, but remains over an order larger than that in *Pnnm*. This test rather clearly favors the selection of *Pnnm.*

7.12. *Bond-length comparison*

Comparison of bond lengths in the two candidate space groups has also been used as a test, on the

assumption that an incorrect choice is likely to result in more outlier values. A basis for such a comparison exists in the accurate determination of the two independent Nb—O distances of 1.8762 (7) and 2.1296 (9) Å in stoichiometric ferroelectric $LiNbO_3$ (average = 2.0029 Å), and of 1.8787 (7) and 2.1264 (8) (average = 2.0026 Å) in congruent ferroelectric $LiNbO_3$, at 298 K (Abrahams & Marsh, 1986). Not many accurately determined Nb—O distances have been reported in centrosymmetric structures; both independent NbO_6 octahedra in $Nb(OCH_3)_5$ (Pinkerton *et al.*, 1976), for example, have two long and four short distances averaging ~2.134 (7) and 1.898 (7) Å, closely comparable to $LiNbO_3$. Nb—O distances in the three independent octahedra of $Sr_5Nb_5O_{17}$, averaged in groups of shorter (s) or longer (l) bonds for both data sets, as refined under all three intensity criteria and each set of weights for the models in either space group, have been deposited as Tables 6(*a*)S and 6(*b*)S. Although the shorter Nb–O distances refined in *Pnnm* are slightly closer to the standard values than those refined in *Pnn*2, the opposite holds for the longer distances. Inspection of the results also shows changes in Nb—O distance distribution within the same space group refined under different intensity conditions.

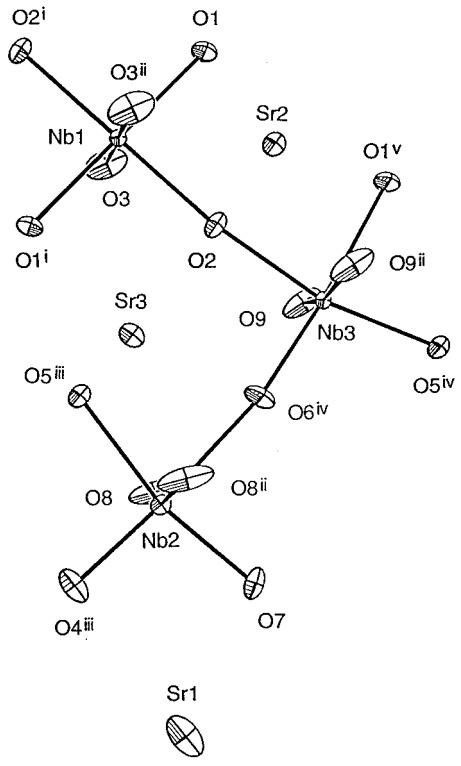

Fig. 3. View of the three symmetry-independent corner-sharing NbO_6 octahedra in $Sr_5Nb_5O_{17}$ for space group *Pnnm* with data set 2 and Type *A*, Type *B* weights, shown with 50% probability displacement ellipsoids (Johnson, 1971). Symmetry codes used in this figure are as given in Table 7.

The bond-length criterion is hence indeterminate and offers no present assistance in selecting the correct space group. A discussion of individual bond lengths refined with data set 2 in *Pnnm* is presented in §10.

7.13. *Atomic displacement*

Among the most direct tests based on diffraction data alone is an examination of the apparent atomic displacements from centrosymmetry, as determined by refinement assuming the noncentrosymmetric space group. Only two atoms in Table 2 and two in Tables 2(*b*)S and 2(*c*)S have $\Delta z > 0.05$ Å on refinement in space group *Pnn*2, see §6. The largest of these apparent displacements from centrosymmetry is less than 0.1 Å, with corresponding r.m.s. thermal or static displacements greater than 0.1 Å. Such a situation is unlikely to be thermodynamically stable long term and a crystal subject to it may be expected to undergo a transition to the centrosymmetric phase. Table 2 and §6 hence offer rather strong evidence in favor of space group *Pnnm*.

7.14. *Atomic thermal or static displacement parameters*

The ADP ellipsoids obtained by refinement with data set 2, condition (iii), and the Type *A* and Type *B* weights in space group *Pnnm* are shown in Fig. 3; those based upon the use of the *SHELXL*96 (Sheldrick, 1996*a*) weights are within ~10% of the former but have s.u.'s between 30 and 50% smaller. The appearance as computed in space group *Pnn*2, either for model I or II, differs from Fig. 3 in two respects. The ellipsoids of many atoms with positive definite ADP's are larger; the most striking difference between the two space groups is related to atoms with n.p.d. ADP's, discussed in detail in §5.4, which cannot be represented by ellipsoids. The many such n.p.d. ADP's formed in *Pnn*2 strongly favor space group *Pnnm*.

In addition to the application of 13 of the 14 tests above based only on the X-ray diffraction data, see also §13, four of the seven physical tests noted below were also applied in the present work.

7.15. *Pyroelectric coefficient measurement*

The upper limit of $p_3 \leq 8$ μC m^{-2} K^{-1} determined for $Sr_5Nb_5O_{17}$ overlaps the smaller values reported for known pyroelectrics (Bhalla & Liu, 1984), although this limit could be considerably reduced if crystals with a larger cross section than those presently available were measured, see §4.1. While the chances are small that a crystal with $p_i \leq 10^{-2}$ μC m^{-2} K^{-1} over its phase stability range would be pyroelectric, the present value is indeterminate regarding the presence or absence of inversion centers.

7.16. *Piezoelectric coefficient measurement*

The measured limit $d_{31} \leq 1\ \mathrm{fC\ N^{-1}}$, see §4.2, is strongly suggestive of a nonpiezoelectric, hence centrosymmetric, crystal since the upper bound is one to two orders of magnitude lower than that reported in any known piezoelectric (Cook, 1984). Piezoelectric coefficients are independent of area, hence crystal sample size is less restrictive than for pyroelectric coefficient measurement.

7.17. *Dielectric hysteresis*

All structurally ferroelectric crystals are expected to exhibit dielectric hysteresis under the appropriate application of an electric field stronger than the coercive field, see *e.g.* Abrahams (1994). Demonstration of hysteresis requires either a single crystal with face areas greater than $\sim$1 mm^2 inclined approximately normal to the polar axis or a polycrystalline plate of area greater than $\sim$5 mm^2. Neither condition could be met with the crystals available, hence this rather definitive measurement could not be made; in addition, the semiconductivity of $Sr_5Nb_5O_{17}$ may make it impossible to attain the necessary field strength.

7.18. *Calorimetry*

The thermal behavior of $Sr_5Nb_5O_{17}$, determined by differential scanning calorimetry in §4.4, provides no evidence for a phase transition below 773 K. This result strongly supports the choice of centrosymmetric space group for $Sr_5Nb_5O_{17}$, see also §7.13.

7.19. *Second harmonic generation*

Determination in §4.3 that the optical second-order nonlinear dielectric susceptibility of $Sr_5Nb_5O_{17}$ is less than 11% that of quartz, *i.e.* $d_{1\mu} < 0.055 \times 10^{-12}\ \mathrm{V^{-1}\ m}$, provides strongly supporting evidence that the crystal possesses inversion centers.

7.20. *Gyration tensor*

All gyration tensor coefficients in point group *mmm* are necessarily zero, whereas $g_{12} \neq 0$ in *mm*2. The High Accuracy Universal Polarimeter, HAUP, based on principles developed by Kobayashi *et al.* (1996), can measure g_{ij} with high sensitivity even in the presence of strong optical dichroism, thereby offering a sensitively discriminating response to the possible absence of inversion centers. The largest crystals available were too small to polish optically into plates with minimum dimensions $\sim 1.5 \times 1.5$ mm^2, as required for the gyration measurements, hence this method could not be used in the present study.

7.21. *Photorefractive determination*

The possibility that the intensity of a laser beam (incoming value less diffraction losses) transmitted through a noncentrosymmetric photorefractive crystal under geometrical conditions similar to those used in holography is greater than that through a centrosymmetric crystal (Woike, 1996) may offer a new method for discriminating between them. The requirement that the test crystal is large enough to form polished parallel plates of optical quality, with minimum edge dimensions $\sim$1.5 mm, for full beam overlap, precluded the use of this test. The second harmonic generation test of §7.19 is expected to be more sensitive for the detection of noncentrosymmetry.

7.22. *Summary and space-group choice*

Nine tests based on diffraction data alone (§7.1, §7.3, §7.4, §7.6, §7.9, §7.10, §7.11, §7.13 and §7.14) are consistent with the choice of space group as *Pnnm* [see also §13 on the use of the program *PLATON* (Spek, 1990), which agrees with these nine test results], four tests (§7.2, §7.5, §7.7 and §7.12) are indeterminate and one (§7.8) was not used. One of the physical tests (§7.15) is indeterminate and three others (§7.17, §7.20 and §7.21) could not be used owing to the small size of the available single crystals. The results of the physical tests in §7.16, §7.18 and §7.19 strongly indicate the correct space group is *Pnnm*. The combined evidence hence rather clearly favors the centrosymmetric choice of space group.

8. Effects of the three intensity criteria on refinement

Fig. 2(*a*) shows that the $N(z)$ cumulative probability distribution for all data closely matches that for a centrosymmetric distribution, see §7.1, whereas the data that remain following the imposition of conditions (i) and (ii), shown in Figs. 2(*b*) and 2(*c*), have distributions for both data sets that match the noncentrosymmetric expectation. Omission of weak and unobserved data can hence result in highly misleading distributions; previous recommendations to use all the measured intensities, see §1, are strongly reinforced by the present study. Table 1 demonstrates the improvement obtainable in the agreement indicators R and $wR(F^2)$ as the limiting condition on the minimum magnitude of $I_{\rm obs}$ is raised, for either choice of space group or weighting model. The ratio of R[F, condition (iii)]/R[(F, condition (i)] in *Pnnm*, for example, is 3.88 [4.69] for data set 1 and 2.77 [2.94] for data set 2; corresponding magnitudes of $wR(F^2)$ give ratios of 1.73 [1.47] and 1.49 [1.16], respectively, where the values in square parentheses are based upon the second set of weights, see §5.1.

The apparent advantages obtained by the imposition of intensity conditions such as (i) or (ii) are clearly illusory in the present work, and perhaps quite generally, with lower R values that surely do not compensate for

the resulting erroneous space-group assignment. The smaller standard uncertainties produced, by factors of 1/1.5 to 1/2 for models I and II in *Pnn*2 compared with those in *Pnnm*, for all but the *z* coordinates are offset by an increase in the latter by as much as a factor of 5 compared with the uncertainties in the *x* and *y* coordinates. Application of the intensity conditions has little effect on the magnitudes of the correlation matrix elements in the presence of Marquart damping for refinement in the noncentrosymmetric space group, but with reduced or no damping these elements increase as dramatically as expected for an incorrect choice of space group with either set of weights applied, see also Watkin (1994).

It may be noted that although data set 2 gives more reliable results than data set 1, as expected, the largest difference between the atomic coordinates refined with data set 1 under condition (iii) and those presented in Table 3 is only 2.0 combined standard uncertainties (c.s.u.) [for x(Sr1)], with only three other differences [y(O1), y(O4) and y(O6)] that exceed 1.0 c.s.u. for the second set of weights. Differences between corresponding ADP's in Tables C1–C4 and those refined with data set 1 under condition (iii) are larger, with U^{12}(O3) at 6.3 c.s.u. followed by U^{11}(O5) at 3.9 c.s.u. and both U^{11}(O4) and U^{33}(O4) at 2.8 c.s.u. All other differences are less than 2.0 c.s.u. The present study confirms the need to consider *all* reflections in cases involving a choice between centrosymmetric and noncentrosymmetric space groups, as pointed out by Schwarzenbach *et al.* (1989), Kassner *et al.* (1993), Marsh (1995) and others.

9. Effects of changing the system of weights

Two different weighting systems were applied in the present least-squares refinements, see §5.1. The first system followed the widely used procedure of *SHELXL*96 (Sheldrick, 1996*a*), hereafter weights 1; the second followed the recommendations of Schwarzenbach *et al.* (1995), hereafter weights 2. A major result of applying weights 2 rather than weights 1 is a significant decrease in $wR(F^2)$. Under intensity condition (iii) in *Pnnm*, for example, with data set 1 and weights 1, $wR(F^2)$ = 0.0967, but with all other conditions held constant except substitution of the use of weights 2, $wR(F^2)$ = 0.0775; similarly, with data set 2 and weights 1, $wR(F^2)$ = 0.0876, but with weights 2, $wR(F^2)$ = 0.0661. The standard deviation of an observation of unit weight S similarly approaches unity more closely on refinement with weights 2 rather than with weights 1; thus, for intensity condition (iii), data set 1 and weights 2, S = 0.856 and for data set 2, S = 0.940, whereas with weights 1, S = 1.240 for set 1 and S = 1.209 for set 2. Further indicator differences on changing from weights 1 to weights 2 are presented in Tables 1 and 1S.

The standard uncertainties in all position coordinates either remain constant or decrease on changing from weights 1 to weights 2, as seen in Table 3. As a consequence, the standard uncertainties of the bond lengths and angles from refinement with weights 2 are also somewhat smaller. The standard uncertainties in all ADP's similarly decrease slightly on using weights 2. Changing the weighting system also changes the resulting residual electron densities; use of weights 2 led to $\Delta\rho_{max}$ and $\Delta\rho_{min}$ values that were reduced by a factor of ~0.8 from those using weights 1 for either data set in either space group. A notable increase in the refinement stability of noncentrosymmetric models I and II was observed with weights 2 compared with the use of weights 1, including fewer refinement cycles being

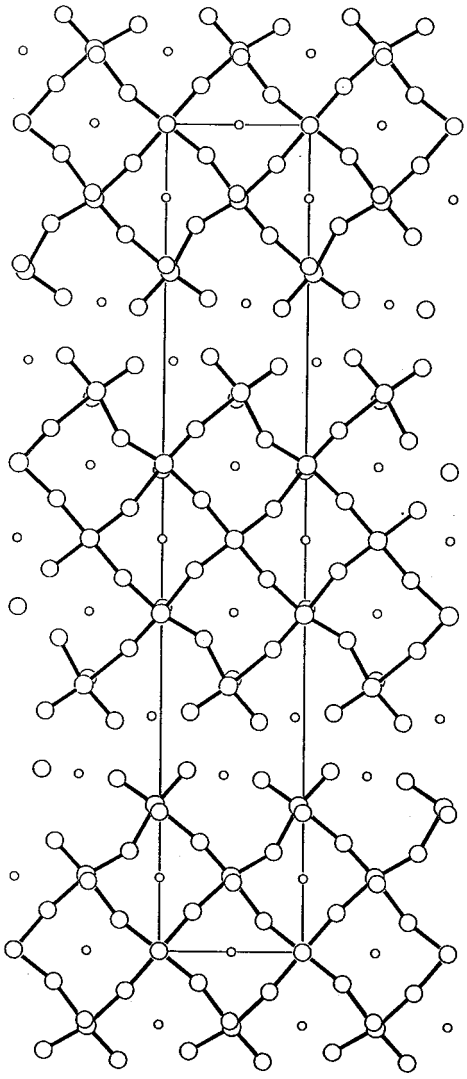

Fig. 4. Content of a unit cell of $Sr_5Nb_5O_{17}$, based on the atomic coordinates in Table 3, viewed along the *c* axis (Keller, 1986). The *a* axis is vertical, Sr is denoted by smaller, Nb by intermediate and O by larger circles.

Table 7. *Selected bond lengths (Å) and angles (°) in centrosymmetric $Sr_5Nb_5O_{17}$*

Corresponds to coordinates in Table 3 based on data set 2 with the first set of weights, followed by values in square parentheses based on the second set of weights, see §5.1 and §5.3. Symmetry codes are not given for the O—Nb—O angles. 90 and 180° angles remain unchanged, hence are given only once.

Nb1—O1	1.969 (4) [1.973 (3)]	Sr2—O1^{vii}	2.669 (3) [2.667 (2)]
Nb1—O1^{i}	1.969 (4) [1.973 (3)]	Sr2—O1	2.669 (3) [2.667 (2)]
Nb1—O3^{ii}	1.9975 (10) [1.9975 (10)]	Sr2—O1^{viii}	2.669 (3) [2.668 (2)]
Nb1—O3	1.9975 (10) [1.9975 (10)]	Sr2—O1^{v}	2.669 (3) [2.668 (2)]
Nb1—O2^{i}	2.030 (4) [2.034 (3)]	Sr2—O9^{viii}	2.711 (5) [2.715 (3)]
Nb1—O2	2.030 (4) [2.034 (3)]	Sr2—O9	2.712 (5) [2.715 (3)]
Nb2—O4^{iii}	1.818 (4) [1.815 (3)]	Sr2—O3	2.837 (1) [2.837 (1)]
Nb2—O7	1.857 (4) [1.857 (3)]	Sr2—O3^{ix}	2.837 (1) [2.837 (1)]
Nb2—O8	2.0214 (13) [2.0219 (11)]	Sr2—O2^{v}	2.954 (3) [2.954 (2)]
Nb2—O8^{ii}	2.0214 (12) [2.0219 (11)]	Sr2—O2^{viii}	2.954 (3) [2.954 (2)]
Nb2—O5^{iii}	2.085 (4) [2.081 (3)]	Sr2—O2	2.954 (3) [2.954 (2)]
Nb2—O6^{iv}	2.277 (4) [2.279 (3)]	Sr2—O2^{vii}	2.954 (3) [2.954 (2)]
Nb3—O6^{iv}	1.844 (4) [1.842 (3)]	Sr3—O5^{iii}	2.544 (3) [2.546 (2)]
Nb3—O5^{iv}	1.952 (4) [1.954 (3)]	Sr3—O5^{x}	2.544 (3) [2.546 (2)]
Nb3—O9	2.0130 (12) [2.0122 (11)]	Sr3—O8	2.614 (4) [2.611 (3)]
Nb3—O9^{ii}	2.0130 (12) [2.0122 (11)]	Sr3—O2^{vii}	2.732 (3) [2.731 (2)]
Nb3—O2	2.044 (4) [2.042 (3)]	Sr3—O2	2.732 (3) [2.732 (2)]
Nb3—O1^{v}	2.173 (4) [2.170 (3)]	Sr3—O9^{xi}	2.785 (5) [2.792 (3)]
Sr1—O7^{vi}	2.465 (2) [2.470 (2)]	Sr3—O3	2.8790 (7) [2.8784 (6)]
Sr1—O7^{iii}	2.465 (3) [2.470 (2)]	Sr3—O9	2.899 (5) [2.890 (3)]
Sr1—O4	2.509 (3) [2.509 (2)]	Sr3—O6^{xii}	2.915 (4) [2.917 (2)]
Sr1—O4^{ii}	2.509 (3) [2.590 (2)]	Sr3—O6^{iv}	2.915 (4) [2.917 (2)]
Sr1—O7	2.539 (5) [2.535 (3)]	Sr3—O1^{i}	3.028 (3) [3.029 (2)]
Sr1—O4^{iii}	2.810 (5) [2.815 (3)]	Sr3—O1^{xiii}	3.028 (3) [3.029 (2)]
Sr1—O8^{iii}	2.907 (6) [2.908 (4)]		

O1—Nb1—O1	180	O7—Nb2—O6	87.8 (2) [87.9 (1)]
O1—Nb1—O3	90 × 4	O8—Nb2—O6	81.7 (2) × 2 [81.6 (1) × 2]
O3—Nb1—O3	180	O5—Nb2—O6	78.9 (2) [79.0 (1)]
O1—Nb1—O2	92.1 (2) × 2 [92.1 (1) × 2]	O6—Nb3—O5	102.0 (2) [101.9 (1)]
O1—Nb1—O2	87.9 (2) × 2 [87.9 (1) × 2]	O6—Nb3—O9	96.6 (2) × 2 [96.4 (1) × 2]
O3—Nb1—O2	90 × 4	O5—Nb3—O9	91.1 (1) × 2 [91.3 (1) × 2]
O2—Nb1—O2	180	O9—Nb3—O9	165.8 (3) [166.1 (2)]
O4—Nb2—O7	97.2 (2) [97.0 (1)]	O6—Nb3—O2	90.8 (2) [90.8 (1)]
O4—Nb2—O8	98.1 (2) × 2 [98.1 (1) × 2]	O5—Nb3—O2	167.2 (2) [167.3 (1)]
O7—Nb2—O8	92.6 (2) × 2 [92.6 (1) × 2]	O9—Nb3—O2	87.4 (1) × 2 [87.3 (1) × 2]
O8—Nb2—O8	162.4 (3) [162.2 (2)]	O6—Nb3—O1	175.2 (2) [175.1 (1)]
O4—Nb2—O5	96.1 (2) [96.1 (1)]	O5—Nb3—O1	82.8 (2) [83.0 (1)]
O7—Nb2—O5	166.7 (2) [166.9 (1)]	O9—Nb3—O1	83.2 (2) × 2 [83.4 (1) × 2]
O8—Nb2—O5	85.6 (1) × 2 [85.5 (1) × 2]	O2—Nb3—O1	84.4 (2) [84.3 (1)]
O4—Nb2—O6	175.0 (2) [175.1 (1)]		

Symmetry codes: (i) $-x+1, -y+1, -z+1$; (ii) $x, y, z+1$; (iii) $-x+\frac{1}{2}, y+\frac{1}{2}, -z+\frac{1}{2}$; (iv) $-x+\frac{1}{2}, y-\frac{1}{2}, -z+\frac{1}{2}$; (v) $-x+1, -y, -z+1$; (vi) $-x+\frac{1}{2}, y+\frac{1}{2}, -z+\frac{3}{2}$; (vii) $x, y, z-1$; (viii) $-x+1, -y, -z$; (ix) $x, y-1, z$; (x) $-x+\frac{1}{2}, y+\frac{1}{2}, -z-\frac{1}{2}$; (xi) $x, y+1, z$; (xii) $-x+\frac{1}{2}, y-\frac{1}{2}, -z-\frac{1}{2}$; (xiii) $-x+1, -y+1, -z$.

necessary as Flack's (1983) x parameter was varied. It may be concluded, on the basis of the present study, that the use of weights derived from Type *A* and Type *B* variances offers many advantages.

10. Structural considerations

Consequent upon the change in space-group assignment of $Sr_5Nb_5O_{17}$ at room temperature from *Pnn*2 to *Pnnm*, see §7.22, is a change in the description of the structure, see Fig. 4, from that given by SWRLWB. The $Nb2O_6$ and $Nb3O_6$ octahedra for Nb2 and Nb3 continue to have a 4 + 1 + 1 distortion, the Nb2—O distances ranging from 1.818 (4) [1.815 (3)] to 2.277 (4) [2.280 (3)] Å and Nb3—O from 1.844 (4) [1.842 (3)] to 2.173 (4) [2.170 (3)] Å, see Table 7. The $Nb1O_6$ octahedron in *Pnnm*, however, is 4 + 2 distorted owing to the special position occupied by O3; it contains two pairs of long Nb1—O distances at 1.998 (1) [1.998 (1)] and 2.030 (4) [2.034 (3)] Å and a short pair of apical distances at 1.969 (4) [1.973 (3)] Å, whereas it appeared to have a 4 + 1 + 1 distortion in *Pnn*2. The Sr–O coordination in *Pnnm* is similar to that refined in *Pnn*2, except for many Sr—O distances that appear independent in the latter but are mirror-related in the former; both NbO_6 octahedra and SrO_{12} cubooctahedra in *Pnnm* exhibit higher symmetry. The

$Sr1O_7$ cation remains quite irregular, with Sr1—O distances ranging from 2.465 (2) [2.470 (2)] to 2.907 (6) [2.908 (4)] Å. Details of the coordination geometry are given in Table 7.

Bond valences calculated with Brown's (1996) *VALENCE* program, using the coordinates in Table 4 as refined with both sets of weights, are given in Table 5S. These parameters, see Brown (1992), confirm the descriptions in §10 of the NbO_6, SrO_7 and SrO_{12} polyhedra. The bond-valence sum for the octahedra is 4.744 (6) [4.710 (5)] v.u. for $Nb1O_6$, 4.925 (7) [4.938 (6)] v.u. for $Nb2O_6$ and 4.803 (7) [4.815 (5)] v.u. for $Nb3O_6$, with a theoretical value of 5 v.u. (valence units). The valence sum of the $Sr1O_7$ polyhedron is 2.074 (2) [2.062 (2)] v.u., increasing to 2.154 (2) [2.142 (2)] v.u. if the longer Sr1—O6, Sr1—O6^{ii} and Sr1—O8 distances are also taken into account. The larger value is consistent with seven-coordination taken as the appropriate description for Sr1. The two SrO_{12} cubooctahedra have valence sums of 2.008 (2) [2.006 (1)] v.u. for Sr2 and 2.090 (2) [2.090 (1)] v.u. for Sr3, hence these coordinations may be accepted as correct.

Comparison of the standard uncertainties in the results obtained either by SWRLWB or by the present refinement in space group *Pnn*2 with those in Table 3 is clearly supportive of the centrosymmetric choice of space group, see also §7.10.

11. Properties of the perovskitic $A_{n+1}B_{n+1}O_{3n+5}$ homologous series

$Sr_5Nb_5O_{17}$ (*i.e.* $SrNbO_{3.4}$) is a member of the homologous series of materials with the general formula $A_{n+1}B_{n+1}O_{3n+5}$ and $n = 4$ crystallizing with a perovskite-related layer structure; determination of its oxygen content by thermogravimetric analysis resulted in the formula $Sr_5Nb_5O_{17.1}$ (Williams *et al.*, 1993; Lichtenberg, Williams *et al.*, 1991). Two other members with $n = 4$ are $CaNbO_{3.4}$ and $LaTiO_{3.4}$ (Williams *et al.*, 1993; Lichtenberg, Williams *et al.*, 1991; Williams *et al.*, 1991; Lichtenberg, Widmer *et al.*, 1991). Three members with $n = 3$ and the formulae $SrNbO_{3.5}$, $CaNbO_{3.5}$ and $LaTiO_{3.5}$ are ferroelectric; their Curie temperatures are among the highest (1600–1850 K) known (Nanamatsu *et al.*, 1975; Nanamatsu *et al.*, 1974; Nanamatsu & Kimura, 1974). Materials with the formulae $SrNbO_x$, $CaNbO_x$ and $LaTiO_x$, for $3.4 < x < 3.5$, display well ordered intergrowths of $n = 3$ and $n = 4$ layers (Williams *et al.*, 1993; Lichtenberg, Williams *et al.*, 1991) and are therefore closer to the pure $n = 3$, *i.e.* $x = 3.5$, noncentrosymmetric structure than to the pure $n = 4$, *i.e.* $x = 3.4$, centrosymmetric structure. Further investigation of electrically conductive oxides in this series with intermediate values of x is necessary to determine if they are noncentrosymmetric, hence possibly ferroelectric, or centrosymmetric.

12. Additional software used

Data collection: Enraf–Nonius *CAD*-4 software (Enraf–Nonius, 1989). Data reduction: *MolEN* (Fair, 1990). Molecular graphics: *SCHAKAL*86 (Keller, 1986). Publication and deposition: *SHELXL*96 (Sheldrick, 1996*a*). Calculation of Type *A* and Type *B* weights: *CORSIG* (Bühler & Schmalle, 1997). Further examination of diffraction data: *PLATON* (Spek, 1990) and *MISSYM* (Le Page, 1987).

13. Concluding remarks

The results obtained from the present case study suggest general strategies to be followed in assigning a space group to a crystal in which the choice between centrosymmetry or noncentrosymmetry is in doubt. It is advisable to apply most, if not all, of the tests outlined in §7.1–§7.14 to the X-ray diffraction data which, preferably, have been obtained by measuring the entire reflection sphere and to which all necessary corrections for absorption, extinction, decay and other systematic sources of error have been applied. Careful allowance for anomalous dispersion is essential. Consideration should be given in the refinement to the use of weights derived from evaluating the Type *A* and Type *B* variances (Schwarzenbach *et al.*, 1995). No reflections should be excluded. In the event that one or more diffraction-based tests present a conclusion contrary to that given by the remaining tests, it is strongly advisable to extend the tests to as many of the seven kinds of physical measurement outlined in §7.15–§7.21 as possible. A positive result from any of the latter tests, if correctly applied, is definitive; negative results require interpretation, but may be given considerable weight if the test is made with high sensitivity.

An observation that may be considered in the process of resolving space-group choices similar to the present choice is the ratio of the number of inorganic crystal structure entries in the Inorganic Crystal Structure Database (Bergerhoff & Brown, 1987) assigned to one of the 68 polar space groups to the total number of entries in the database. The June 1995 database release had a ratio of 8.2% (Abrahams, 1996*b*). While this ratio does not necessarily mirror nature unambiguously, owing to difficulties associated with structure solution among other possible causes, it probably does not differ widely from the actual value. The chance that a given inorganic crystal belongs to a polar rather than to a centrosymmetric space group may hence be considered unlikely to be much larger than approximately 1 in 10.

Following CIF submission of data sets 1 and 2 to the editorial staff in Chester, further examination by means of the program *PLATON* (Spek, 1990), in which an extended version of *MISSYM* (Le Page, 1987) is implemented, was rather strongly found to favor the

possibility of inversion centers being present in the structure. This test should hence be added to the 14 discussed in §7.1–§7.14. *MISSYM* (Le Page, 1987) further indicated the presence of a pseudobody-centered cell, as noted previously by SWRLWB. However, ∼20% of the total number of $I(hkl)$ are present both with high statistical significance and $h + k + l = 2n + 1$, providing unambiguous evidence that the unit cell is primitive.

It is a pleasure to thank Professor G. M. Sheldrick and Dr H. D. Flack for valuable correspondence, Professor W. Baur for helpful discussions of his distributional test, Professor J. Kobayashi for offering to measure the gyration tensors, the late Professor V. Schomaker and Dr R. E. Marsh for stimulating discussions of the complexities associated with establishing small deviations from centrosymmetry, Professor I. D. Brown for a copy of his *VALENCE* program, Dr A. Linden and R. Pellaux for calculating the $N(z)$ cumulative probability distributions, Professor V. Gramlich and Dr M. Estermann for help with calculations, R. Bühler for programming, the Alexander von Humboldt Foundation for an extension of the Humboldt Prize awarded earlier to one of us (SCA) during which this work was begun, and the National Science Foundation (DMR-9708246) for support.

References

Abrahams, S. C. (1969). *Acta Cryst.* A**25**, 165–173.
Abrahams, S. C. (1972). *J. Appl. Cryst.* **5**, 143.
Abrahams, S. C. (1975). *Anomalous Scattering*, edited by S. Ramaseshan & S. C. Abrahams, pp. 199–221. Copenhagen: Munksgaard.
Abrahams, S. C. (1994). *Acta Cryst.* A**50**, 658–685.
Abrahams, S. C. (1996*a*). *Acta Cryst.* A**52**, 790–805.
Abrahams, S. C. (1996*b*). *Acta Cryst.* A**52**, C-388.
Abrahams, S. C. & Marsh, P. (1986). *Acta Cryst.* B**42**, 61–68.
Baur, W. H. & Tillmanns, E. (1986). *Acta Cryst.* B**42**, 95–111.
Bergerhoff, G. & Brown, I. D. (1987). *Crystallographic Databases*, edited by F. H. Allen, G. Bergerhoff & R. Sievers. International Union of Crystallography.
Bhalla, A. S. & Liu, S. T. (1984). *Landholdt–Börnstein, New Series, Group III, Vol. 18. Elastic, Piezoelectric, Pyroelectric, Piezooptic, Electrooptic Constants and Nonlinear Dielectric Susceptibilites of Crystals*, edited by K.-H. Hellwege & A. M. Hellwege, pp. 325–358. Berlin: Springer-Verlag.
Brown, I. D. (1992). *Acta Cryst.* B**48**, 553–572.
Brown, I. D. (1996). *J. Appl. Cryst.* **29**, 479–480.
Brünger, A. T. (1992). *Nature*, **355**, 472–475.
Brünger, A. T. (1993). *Acta Cryst.* D**49**, 24–36.
Bühler, R. & Schmalle, H. (1997). *CORSIG*97. *A Fortran Program for the Calculation of Combined Standard Uncertainties Based on Type A and Type B Variances*. University of Zürich, Switzerland.
Cook, W. R. (1984). *Landholdt–Börnstein, New Series, Group III, Vol. 18. Elastic, Piezoelectric, Pyroelectric, Piezooptic, Electrooptic Constants and Nonlinear Dielectric Susceptibilites of Crystals*, edited by K.-H. Hellwege & A. M. Hellwege, pp. 180–325. Berlin: Springer-Verlag.
Dougherty, J. P. & Kurtz, S. K. (1976). *J. Appl. Cryst.* **9**, 145–158.
Engelhard, Inc. (1995). Newark, NJ.
Enraf–Nonius (1989). *CAD*-4 *Software*. Enraf–Nonius, Delft, The Netherlands.
Fair, C. K. (1990). *MolEN. An Interactive Intelligent System for Crystal Structure Analysis*. Enraf–Nonius, Delft, The Netherlands.
Flack, H. D. (1983). *Acta Cryst.* A**39**, 876–881.
Flack, H. D. (1996). Private communication.
Hamilton, W. C. (1965). *Acta Cryst.* **18**, 502–510.
Howells, E. R., Phillips, D. C. & Rogers, D. (1950). *Acta Cryst.* **3**, 210–214.
Jerphagnon, J., Kurtz, S. K. & Oudar, J.-L. (1984). *Landholdt–Börnstein, New Series, Group III, Vol. 18. Elastic, Piezoelectric, Pyroelectric, Piezooptic, Electrooptic Constants and Nonlinear Dielectric Susceptibilites of Crystals*, edited by K.-H. Hellwege & A. M. Hellwege, pp. 456–506. Berlin: Springer-Verlag.
Johnson, C. K. (1971). *ORTEP*II. Report ORNL-3794. Oak Ridge National Laboratory, Oak Ridge, TN 37830, USA.
Kassner, D., Baur, W. H., Joswig, W., Eichhorn, K., Wendschuh-Josties, M. & Kupčik, V. (1993). *Acta Cryst.* B**49**, 646–654.
Keller, E. (1986). *SCHAKAL*86. *Fortran Program for the Graphic Representation of Molecular and Crystallographic Models*. University of Freiburg, Germany.
Kobayashi, J., Asahi, T., Sakurai, M., Takahashi, M., Okubo, K. & Enomoto, Y. (1996). *Phys. Rev. B*, **53**, 11784–11795.
Kurtz, S. K. & Perry, T. T. (1968). *J. Appl. Phys.* **39**, 3798–3813.
Le Page, Y. (1987). *J. Appl. Cryst.* **20**, 264–269.
Lichtenberg, F., Widmer, D., Bednorz, J. G., Williams, T. & Reller, A. (1991*a*). *Z. Phys. B*, **82**, 211–216.
Lichtenberg, F., Williams, T., Reller, A., Widmer, D. & Bednorz, J. G. (1991*b*). *Z. Phys. B*, **84**, 369–374.
Marsh, R. E. (1981). *Acta Cryst.* B**37**, 1985–1988.
Marsh, R. E. (1995). *Acta Cryst.* B**51**, 897–907.
Marsh, R. E. (1996). Private communications.
Nanamatsu, S. & Kimura, M. (1974). *J. Phys. Soc. Jpn*, **36**, 1495.
Nanamatsu, S., Kimura, M., Doi, K., Matsushita, S. & Yamada, N. (1974). *Ferroelectrics*, **8**, 511–513.
Nanamatsu, S., Kimura, M. & Kawamura, T. (1975). *J. Phys. Soc. Jpn*, **38**, 817–824.
Pinkerton, A. A., Schwarzenbach, D., Hubert-Pfalzgraf, L. G. & Riess, J. G. (1976). *Inorg. Chem.* **15**, 1196–1199.
Schmalle, H. W., Williams, T., Reller, A., Lichtenberg, F., Widmer, D. & Bednorz, J. G. (1995). *Acta Cryst.* C**51**, 1243–1246.
Schomaker, V. (1996). Private communications.
Schomaker, V. & Marsh, R. E. (1979). *Acta Cryst.* B**35**, 1933–1934.
Schwarzenbach, D., Abrahams, S. C., Flack, H. D., Gonschorek, W., Hahn, Th., Huml, K., Marsh, R. E., Prince, E., Robertson, B. E., Rollett, J. S. & Wilson, A. J. C. (1989). *Acta Cryst.* A**45**, 63–75.
Schwarzenbach, D., Abrahams, S. C., Flack, H. D., Prince, E. & Wilson, A. J. C. (1995). *Acta Cryst.* A**51**, 565–569.

Sheldrick, G. M. (1996*a*). *SHELXL*96. Beta Version 03. University of Göttingen, Germany.
Sheldrick, G. M. (1996*b*). Private communications.
Spek, A. L. (1990). *Acta Cryst.* A**46**, C-34.
Tolédano, J.-C. & Tolédano, P. (1987). *The Landau Theory of Phase Transitions*. Singapore: World Scientific.
Watkin, D. (1994). *Acta Cryst.* A**50**, 411–437.
Williams, T., Lichtenberg, F., Widmer, D., Bednorz, J. G. & Reller, A. (1993). *J. Solid State Chem.* **103**, 375–386.
Williams, T., Schmalle, H., Reller, A., Lichtenberg, F., Widmer, D. & Bednorz, J. G. (1991). *J. Solid State Chem.* **93**, 534–548.
Woike, Th. (1996). Paul-Scherrer Institut Proceedings 96–02. Paul-Scherrer Institut, Villigen, Switzerland.